Malaysian Journal of Mathematical Sciences 15(1): 125–136 (2021)

MALAYSIAN JOURNAL OF MATHEMATICAL SCIENCES

Journal homepage: http://einspem.upm.edu.my/journal

Convective Mass and Heat Transfer of Sakiadis Flow of Magnetohydrodynamic Casson Fluid Over a Horizontal Surface Employing Cattaneo-Christov Heat Flux Model

Asmadi, M. S.[1], Siri, Z. *[1], and Kasmani, R. M.[2]

[1] *Institute of Mathematical Sciences, Faculty of Science, University of Malaya, 50603, Kuala Lumpur, Malaysia*
[2] *Mathematics Division, Center for Foundation Studies in Sciences, University of Malaya, 50603, Kuala Lumpur, Malaysia*

E-mail: zailansiri@um.edu.my
* *Corresponding author*

Received: 21 January 2020
Accepted: 19 November 2020

ABSTRACT

Convective mass and heat transfer study of Sakiadis flow of magnetohydrodynamic Casson fluid past a horizontal plate is produced in this article by employing the Cattaneo-Christov heat flux model. The governing equations are transformed into a set of ordinary differential equation by applying some similarity variables. A standard second-order and a variation of third-order finite difference method are employed to find the effect of the magnetic force on the fluid system using a local similarity approach. The variation in the boundary layer with the parameters present in the problem is discussed in detail in this paper. Several dimensional forms of the system are provided and the heat map of the thermal boundary layer with different parameters are investigated further in this article. Based on the analysis, the higher the Casson parameter in the system, the lower the velocity of the fluid while the temperature and the concentration increase.

Keywords: Magnetohydrodynamic, Casson fluid, Heat and mass transfer, Cattaneo-Christov heat flux model, Sakiadis flow

1. Introduction

There are two types of fluids in our daily life; Newtonian and non-Newtonian fluids. The non-Newtonian fluids attracted a lot of interests and have been ongoing research among scientific communities due to its useful application in many aspects of the industry. Toothpaste, ketchup, saliva and human blood are several examples of the said fluid. Since the non-Newtonian fluid model consists of complex characteristics, there does not exist a single equation to constitute all the characteristics of the fluid. A typical non-Newtonian fluid model may only capture one or two aspects of the fluid, so researchers will choose the model that suits the most to their research analysis. Because of these limitations, several researchers developed non-Newtonian fluid models to capture different characteristics of the model and are divided into several categories. Some fluid model is more useful for certain application than others. Casson fluid captures the aspect of the yield stress of the fluid which was proposed by Casson (1959) in his study on the flow of the pigment oil suspensions of the printing ink. It is also the most common rheological model used in engineering and industries since this area deals with a lot of fluids with the yield stress characteristics. Several researches prior to the present study have been done by Mukhopadhyay (2013), Arthur et al. (2015), Animasaun et al. (2016), Malik et al. (2016), Raju et al. (2017) and Mythili et al. (2017).

Mass and heat transfer exists in many instances in industrial processes such as heat conduction in mobile smartphones, human tissues, and water heater. Heat transfer is a phenomenon in which the differences in temperature causes energy transfer between some medium. The idea of the study of heat transfer characteristics has been revolved around the well-known Fourier Law of heat conduction for quite some time. This simplistic law may be used for a simple system but is not suitable for a more complex set up. The downside of this law is a small disturbance will affect the fluid instantly due to the parabolic type energy equation that the law produced. Cattaneo (1948) modified the law since he thought the law is somewhat unrealistic physically from the above standpoint of view. So, he includes a relaxation time for heat flux, which was further refined by Christov (2009) by employing the Oldroyd-B's upper convective derivatives. This new heat flux model is a generalization over the Fourier Law of heat conduction. The study of several types of fluids governing by Cattaneo-Christov heat flux model has been done by researchers such as Han et al. (2014), Abbasi et al. (2015), Khan et al. (2015), Hayat et al. (016a),Waqas et al. (2016), Sui et al. (2016), Mushtaq et al. (2016) and Vinod et al. (2017).

The objective of this article is to analyse numerically the mass and heat transfer rate in Magnetohydrodynamic (MHD) Casson fluid with Sakiadis flow. The heat transfer is analysed using the Cattaneo-Christov heat flux model as opposed to the classical Fourier Law. The resulting velocity, temperature and concentration gradient profile are computed using the finite difference method (FDM). The dimensionless parameter associated with the problems are varied accordingly to see the effect of variation, and the results are discussed in the graphical form. The novelty of this paper is the usage of Cattaneo-Christov heat flux model in investigating the behavior of the fluid flow as well as the heat and mass transfer of MHD Casson fluid employing Sakiadis flow past a flat plate. Previous researches uses the Fourier law of heat conduction, which is a simple heat transfer model. Since the application of heat transfer knowledge is vastly applied in the industries and manufacturing processes, the model is too simple to capture the behavior of the fluid. By including the relaxation time for heat flux, the fluid behavior can be observed in detail.

2. Mathematical Formulation

The laminar, two-dimensional set up of MHD Casson fluid over a semi-infinite positive plane at $y = 0$ is considered as shown in Figure 1. An assumption is made by assuming the plate has a constant temperature T_w, constant concentration C_w, ambient fluid temperature T_∞ and ambient concentration C_∞. For the purpose of this problem, the fluid is incompressible and electrically conducting.

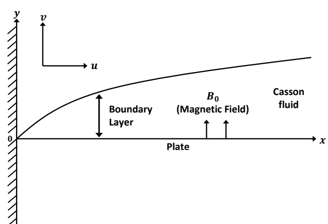

Figure 1: Geometry representation of the fluid

The rheological equation for a non-Newtonian fluid is defined as,

$$\tau = \tau_0 + \mu\alpha^*, \tag{1}$$

where τ is the Cauchy stress tensor, μ is the dynamic viscosity of the fluid under consideration and α^* is the shear rate. Equivalently, for Casson fluid, Eq.(1) can be expanded as,

$$\tau_{ij} = \begin{cases} 2\left(\mu_B + \dfrac{p_y}{\sqrt{2\pi}}\right) e_{ij}, & \pi > \pi_c \\ \\ 2\left(\mu_B + \dfrac{p_y}{\sqrt{2\pi_c}}\right) e_{ij}, & \pi < \pi_c \end{cases} \tag{2}$$

where $\pi = e_{ij}e_{ji}$ with e_{ij} is the $(i,j)^{th}$ component of the fluid deformation rate, $p_y = \dfrac{\mu_B\sqrt{2\pi}}{\beta}$ is the yield stress of the Casson fluid, μ_B is the dynamic viscosity of the Casson fluid,π_c is the critical value of π and β is the Casson fluid parameter.

The governing equations of steady Sakiadis flow of an incompressible MHD Casson fluid are:

$$\frac{\partial u}{\partial x} + \frac{\partial v}{\partial y} = 0, \tag{3}$$

$$u\frac{\partial u}{\partial x} + v\frac{\partial u}{\partial y} = \nu\left(1 + \frac{1}{\beta}\right)\frac{\partial^2 u}{\partial y^2} - \frac{\sigma \mathrm{B}_0^2}{\rho}u, \tag{4}$$

$$u\frac{\partial T}{\partial x} + v\frac{\partial T}{\partial y} + \lambda_2 \left[\begin{array}{c} u^2\dfrac{\partial^2 T}{\partial x^2} + v^2\dfrac{\partial^2 T}{\partial y^2} + 2uv\dfrac{\partial^2 T}{\partial x \partial y} + \\ \left(u\dfrac{\partial u}{\partial x} + v\dfrac{\partial u}{\partial y}\right)\dfrac{\partial T}{\partial x} + \left(u\dfrac{\partial v}{\partial x} + v\dfrac{\partial v}{\partial y}\right)\dfrac{\partial T}{\partial y} \end{array}\right] = \alpha\frac{\partial^2 T}{\partial y^2}. \tag{5}$$

$$u\frac{\partial C}{\partial x} + v\frac{\partial C}{\partial y} = D\frac{\partial^2 C}{\partial y^2}, \tag{6}$$

where x is the coordinate along the semi-infinite plane, y is the coordinate normal to the surface of the plate, u and v are the velocity components along the x and y axis respectively, ν is the fluid kinematic viscosity, ρ is the density of the fluid, σ is the electrical conductivity of the fluid, B_0 is the magnetic field in the direction of normal to the horizontal surface, β is the Casson parameter, C_p is the heat capacity, T is the local temperature of the fluid, D is the mass diffusion coefficient and C the local mass concentration. The boundary conditions for

Sakiadis flow are,

$$\begin{aligned} &u = U, v = 0, T = T_w, C = C_w \quad &&\text{at } y = 0, \\ &u \to 0, T \to T_\infty, C \to C_\infty &&\text{as } y \to \infty. \end{aligned} \tag{7}$$

To solve Eqs.(4), (5) and (6), the following similarity transformation is used,

$$\begin{gathered} \eta = y\sqrt{\frac{U}{\nu x}}, \quad u = Uf'(\eta), \quad v = -\frac{1}{2}\sqrt{\frac{U\nu}{x}}(f - \eta f'), \\ \theta = \frac{T - T_\infty}{T_w - T_\infty}, \quad \phi = \frac{C - C_\infty}{C_w - C_\infty}. \end{gathered} \tag{8}$$

By the above transformation, Eq.(3) is satisfied unconditionally. Using transformation (8), Eqs.(4), (5) and (6) are then transformed into the following:

$$\left(1 + \frac{1}{\beta}\right) f''' + \frac{1}{2} f f'' - \mathrm{M} f' = 0, \tag{9}$$

$$\frac{1}{\mathrm{Pr}}\theta'' + \frac{1}{2} f\theta' - \frac{\gamma}{2}\left(3ff'\theta' + f^2\theta''\right) = 0, \tag{10}$$

$$\phi'' + \frac{\mathrm{Sc}}{2} f\phi' = 0. \tag{11}$$

By using the same transformation, the boundary conditions (7) are reduced into the following:

$$\begin{gathered} f(0) = 0, \quad f'(0) = 0, \quad f \to 1 \quad \text{as} \quad \eta \to \infty, \\ \theta(0) = 1, \quad \theta \to 0 \quad \text{as} \quad \eta \to \infty, \\ \phi(0) = 1, \quad \phi \to 0 \quad \text{as} \quad \eta \to \infty. \end{gathered} \tag{12}$$

where $\beta = \dfrac{\mu_B\sqrt{2\pi_c}}{p_y}$ is the Casson parameter, $\mathrm{M} = \dfrac{\sigma \mathrm{B}_0^2 x}{U\rho}$ is the magnetic field parameter or Hartmann number, $\mathrm{Pr} = \dfrac{\nu}{\alpha}$ is the Prandtl number, $\gamma = \dfrac{\lambda_2 U}{2x}$ is the local Deborah number for temperature and $\mathrm{Sc} = \dfrac{\nu}{D}$ is the Schmidt number.

Since the parameters M and γ contains the function of x, the local similarity solutions are used instead, and the local solution found can be used to see the effect of parameters on the system.

3. Results and Discussion

To solve the nonlinear boundary value problem (9), a newly developed finite difference method (FDM) that was proposed by Pandey (2017) was used. For Eqs. (10) and (11) the method which presented by Burden and Faires (2011) was employed. All computations were done with a tolerance of $\epsilon = 10^{-5}$.

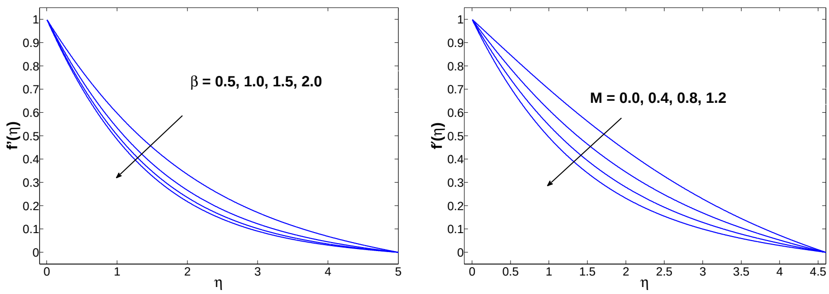

Figure 2: The fluid velocity gradient for several values of: (a) β when $M = 0.5$ (left); (b) M when $\beta = 0.5$ (right); with Pr = Sc = 1 and $\gamma = 0.5$

Figure 2a shows the fluid velocity profile for some Casson parameter. As β increases, the fluid velocity decreases. This means as the fluid tends to behave like the Newtonian fluid, i.e. $\beta \to \infty$, the magnitude of fluid velocity decreases. Consequently, this produces a thinner momentum boundary layer of the fluid. This also means that the Newtonian-behaviour fluid will produce a thinner momentum boundary layer than Casson-behaviour fluid. Figure 2b presents the fluid velocity profile for some Hartmann number. From Figure 2b, the fluid velocity decreases as M increases significantly. As M increases, the velocity of the Casson fluid is disturbed by the Lorenz force present in the fluid and thus helps the fluid to move faster, and in turns, produce a thinner momentum boundary layer. It can be concluded that the higher the Hartmann number, the thinner the momentum boundary layer.

The effect of Casson parameter on the fluid temperature gradient is shown in Figure 3a. Based on the Figure 3a, as β increases, the fluid temperature gradient increases insignificantly. This means as the fluid behaves more like Newtonian fluid (as $\beta \to \infty$), the thermal boundary layer becomes thicker and produce a lower rate of the heat dissipation in the system. It can be concluded that the fluid that behaves like Casson behaviour has a higher heat dissipation than Newtonian-like fluid. Figure 3b presents the effect of Hartmann number on the fluid temperature. In Figure 3b, as M increases, the Casson fluid temperature gradient increases. Since the presence of the magnetic field in the

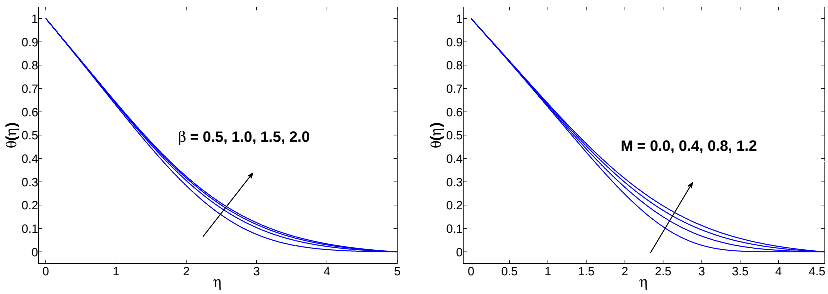

Figure 3: The fluid temperature gradient for several values of: (a) β when $M = 0.5$(left); (b) M when $\beta = 0.5$(right); with Pr = Sc = 1 and $\gamma = 0.5$

system produces Lorenz force, this causes the said force to disturb the heat dissipation of the fluid by retarding the rate of the heat transfer in the fluid. This causes the thermal boundary layer to become thicker as M increases.

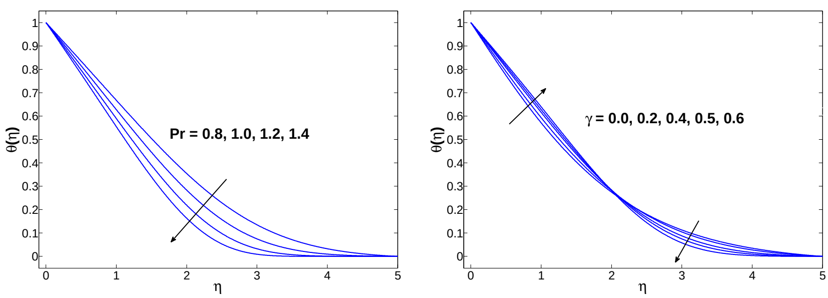

Figure 4: The fluid temperature gradient for several values of: (a) Pr when $\gamma = 0.5$ (left); (b) γ when Pr= 1 (right); with $\beta =$ M = 0.5 and Sc= 0.5

Figure 4a presents the effect of Prandtl number on the fluid temperature. As the value of Pr increases, the temperature gradient of the fluid decreases. As Pr increases, the momentum diffusivity increases and dominates the thermal diffusivity. The fluid velocity is high enough to help the heat transfer of the fluid. This, makes the heat dissipation rate faster and makes the boundary layer to become thinner. It can be seen that Figure 4b shows the effect of the local Deborah number, γ on the fluid temperature gradient. The temperature gradient of the system increases at first, but later at $\eta \approx 2$, the temperature gradient drops when the value of gamma rises. From this observation, it can be noted that the heat transfer relaxation time of the fluid increases, which produces a thinner boundary layer of the fluid. This illustrates that the dissipation of heat occurs at a faster rate.

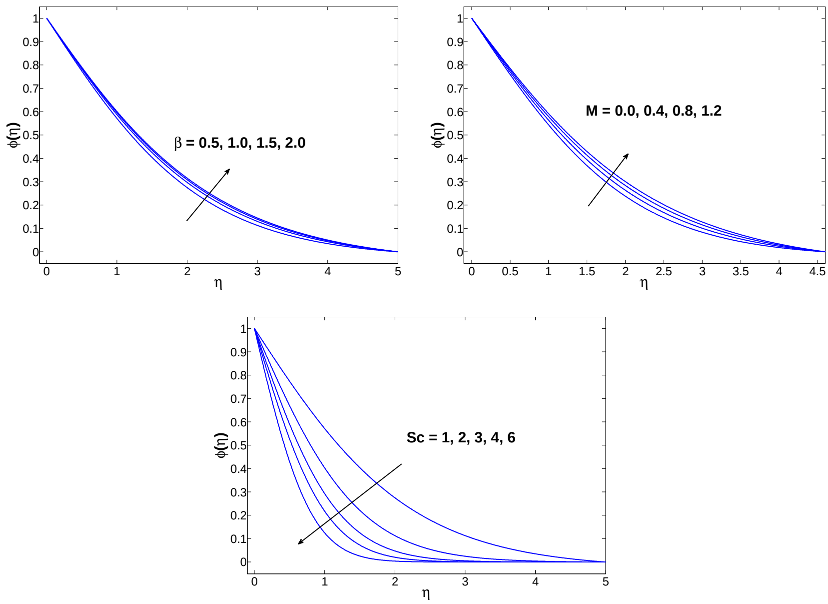

Figure 5: The fluid concentration gradient for several values of: (a) β when $M = 0.5$ and $\mathrm{Sc} = 1$ (top, left); (b) M when $\beta = 0.5$ and $\mathrm{Sc} = 1$ (top, right); (c) Sc when $\beta = M = 0.5$ (bottom); with $\mathrm{Pr} = 1$ and $\gamma = 0.5$

The effect of Casson parameter to the fluid concentration gradient is shown in Figure 5a. As β rises, the concentration gradient increases insignificantly. This means as the fluid employs more of the characteristics of a Newtonian fluid (as $\beta \to \infty$), the concentration boundary layer to become thicker and produce a low mass transfer rate. It can be concluded that the fluid that behaves like Casson behaviour has a higher mass transfer rate than Newtonian-like fluid. Figure 5b shows the effect of the magnetic force on the concentration gradient of the fluid. Since magnetic field strength in the system is represented by the Hartmann number in the system, as M increases, the fluid concentration gradient increases. This is because the presence of the magnetic fields through Lorenz force retards the mass transfer rate of the fluid by applying opposite force. This causes the concentration boundary layer becomes thicker as M increases. The effect of the Schmidt number onto the fluid mass distribution is shown in Figure 5c. It can be seen from Figure 5c that as Sc increases, the concentration gradient decrease. It means that the higher ratio of fluid momentum diffusivity and fluid mass diffusivity in the system resulted in a thinner boundary layer of mass transfer.

Table 1: The physical properties for selected fluid

Fluid	Pr	$T_\infty(^\circ C)$	ν (cm^2/s)
Gaseous ammonia	1.5-2	25	0.145

The dimensional form for some type of system is presented for a better understanding of the results produced earlier. Table 1 presents the physical properties of fluid used to demonstrate the system in a real-world situation. Figure 6 showed the heat map of gaseous ammonia at a constant T_∞, T_w, U_∞, M, γ and Sc, with $\beta = 0.5$ for Figure 6a and $\beta = 2.0$ for Figure 6b. It can be shown from Figure 6 that the thermal boundary layer for $\beta = 0.5$ is thinner than $\beta = 2.0$. Based on the Figure 6, it can be concluded that as the Casson parameter increases, it produce a thicker thermal boundary layer, which means the heat dissipation rate decreases. This result strengthens the result found in Figure 2a.

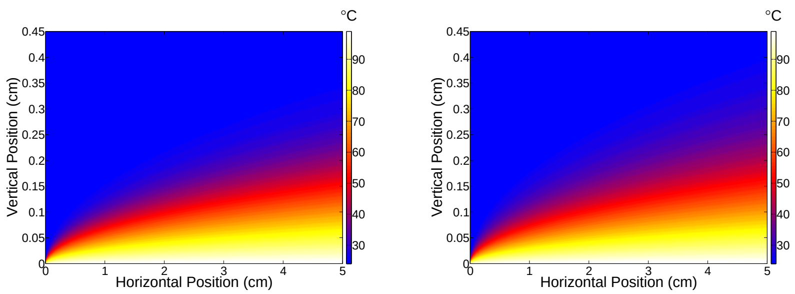

Figure 6: The heat map of gaseous ammonia with: (a) $\beta = 0.5$; (b) $\beta = 2.0$; at $T_\infty = 25^\circ C$ with $U_\infty = 100$ cm/s, $T_w = 100^\circ C$, M= $\gamma = 0.5$ and Sc= 1

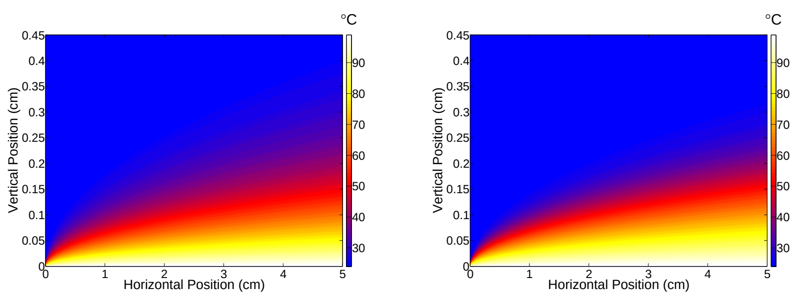

Figure 7: The heat map of gaseous ammonia with: (a) $\gamma = 0.0$; (b) $\gamma = 0.6$; at $T_\infty = 25^\circ C$ with $U_\infty = 100$ cm/s, $T_w = 100^\circ C$, M= $\beta = 0.5$ and Sc= 1

Figures 7 presented the heat map of Sakiadis flow for gaseous ammonia at a constant T_∞, T_w, U_∞, β, M and Sc, with $\gamma = 0.0$ for Figure 7a and $\gamma = 0.6$ for Figure 7b. Noted that $\gamma = 0.0$ corresponds to the classical simplistic Fourier law heat transfer model. Based on the heat map shown in Figures 7a and 7b, the thermal boundary layer for $\gamma = 0.0$ is thicker than that for $\gamma = 0.6$. This means that when the fluid behaves like Fourier law model, the heat dissipation is not as efficient as Cattaneo-Christov heat flux model. In conclusion, Cattaneo-Christov heat flux model increase the efficiency of heat dissipation in the system. This observation is in match with the analysis from Figure 4b.

4. Conclusion

This article discusses the convective mass and heat transfer of Sakiadis fluid flow of Magnetohydrodynamic Casson fluid over a horizontal surface by employing Cattaneo-Christov heat flux model. The summary of the work is listed below:

1. The higher Casson parameter causes the velocity profile to decrease but vice versa for the temperature and the concentration profile.
2. As the Hartmann number increases, the lower the fluid velocity in the system but the temperature and concentration of the fluid increase.
3. Increasing the local Deborah number for temperature produce the lower temperature gradient of the fluid.
4. The higher the Prandtl number, the lower the temperature gradient of the fluid.
5. For a higher Schmidt number, the fluid concentration gradient in the system decreases.
6. The boundary layer thickness decreases with the increase of the local Deborah number for temperature but produce a thicker boundary layer with the increase of the Casson parameter.

Acknowledgement

The authors express their gratitude towards the Ministry of Education Malaysia and University of Malaya for the support given financially through

Fundamental Research Grant Scheme FP043-2017A and University of Malaya Research Grant RG397-17AFR.

References

Abbasi, F., Mustafa, M., Shehzad, S., Alhuthali, M., and Hayat, T. (2015). Analytical study of Cattaneo-Christov heat flux model for a boundary layer flow of Oldroyd-B fluid. *Chinese Physics B*, 25(1):1–6.

Animasaun, I. L., Adebile, E. A., and Fagbade, A. I. (2016). Casson fluid flow with variable thermo-physical property along exponentially stretching sheet with suction and exponentially decaying internal heat generation using the homotopy analysis method. *Journal of the Nigerian Mathematical Society*, 35:1–17.

Arthur, E. M., Seini, I. Y., and Bortteir, L. B. (2015). Analysis of Casson fluid flow over a vertical porous surface with chemical reaction in the presence of magnetic field. *Journal of Applied Mathematics and Physics*, 03(06):713–723.

Burden, R. L. and Faires, J. D. (2011). *Numerical Analysis*. Boston, USA: Cengage Learning.

Casson, N. (1959). Flow equation for pigment oil suspensions of the printing ink type. *Rheology of Disperse Systems*, (1959):84–102.

Cattaneo, C. (1948). Sulla Conduzione del Calore. *Atti del Seminario Matematico e Fisico dell' Universitá di Modena*, 3:83–101.

Christov, C. I. (2009). On frame indifferent formulation of the Maxwell-Cattaneo model of finite-speed heat conduction. *Mechanics Research Communications*, 36(4):481–486.

Han, S., Zheng, L., Li, C., and Zhang, X. (2014). Coupled flow and heat transfer in viscoelastic fluid with Cattaneo-Christov heat flux model. *Applied Mathematics Letters*, 38:87–93.

Hayat, T., Muhammad, T., Al-Mezal, S., and Liao, S. (2016a). Darcy-Forchheimer flow with variable thermal conductivity and Cattaneo-Christov heat flux. *International Journal of Numerical Methods for Heat and Fluid Flow*, 26(8):2355–2369.

Khan, J. A., Mustafa, M., Hayat, T., and Alsaedi, A. (2015). Numerical study of Cattaneo-Christov heat flux model for viscoelastic flow due to an exponentially stretching surface. *PLoS ONE*, 10(9):1–10.

Malik, M. Y., Khan, M., Salahuddin, T., and Khan, I. (2016). Variable viscosity and MHD flow in Casson fluid with Cattaneo Christov heat flux model: Using Keller Box method. *Engineering Science and Technology, an International Journal*, 19(4):1985–1992.

Mukhopadhyay, S. (2013). Casson fluid flow and heat transfer over a nonlinearly stretching surface. *Chinese Physics B*, 22(7):1–5.

Mushtaq, A., Abbasbandy, S., Mustafa, M., Hayat, T., and Alsaedi, A. (2016). Numerical solution for Sakiadis flow of upper-convected Maxwell fluid using Cattaneo-Christov heat flux model. *AIP Advances*, 6(1). https://doi.org/10.1063/1.4940133.

Mythili, D., Sivaraj, R., and Rashidi, M. M. (2017). Heat generating/absorbing and chemically reacting Casson fluid flow over a vertical cone and flat plate saturated with non-Darcy porous medium. *International Journal of Numerical Methods for Heat and Fluid Flow*, 27(1):156–173.

Pandey, P. K. (2017). A numerical method for the solution of general third order boundary value problem. *Bulletin of the International Mathematical Virtual Institute*, 7:129–138.

Raju, R. S., Reddy, B. M., and Reddy, G. J. (2017). Finite element solutions of free convective Casson fluid flow past a vertically inclined plate submitted in magnetic field in presence of heat and mass transfer. *International Journal of Computational Methods in Engineering Science and Mechanics*, 18(4-5):250–265.

Sui, J., Zheng, L., and Zhang, X. (2016). Boundary layer heat and mass transfer with Cattaneo-Christov double-diffusion in upper-convected Maxwell nanofluid past a stretching sheet with slip velocity. *International Journal of Thermal Sciences*, 104:461–468.

Vinod, G., Raju, C. S. K., Fatima, R., and Varma, S. V. K. (2017). Heat transfer analysis of Blasius and Sakiadis flow of MHD radiated Maxwell fluid with Cattaneo-Christov heat flux model. *International Journal of Research in Science and Engineering*, Special Issue(March):198–206.

Waqas, M., Hayat, T., Farooq, M., Shehzad, S. A., and Alsaedi, A. (2016). Cattaneo-Christov heat flux model for flow of variable thermal conductivity generalized Burgers' fluid. *Journal of Molecular Liquids*, 220:642–648.